www.ietdl.org

Published in IET Radar, Sonar and Navigation
Received on 20th October 2012
Revised on 26th August 2013
Accepted on 11th September 2013
doi: 10.1049/iet-rsn.2013.0017

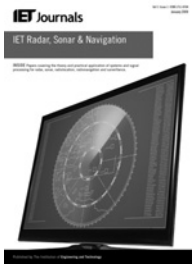

ISSN 1751-8784

Joint mode identification and localisation improvement of over-the-horizon radar with forward-based receivers

Xiaoxue Feng, Yan Liang, Lin Zhou, Lianmeng Jiao, Zengfu Wang

School of Automation, Northwestern Polytechnical University, Xi'an 710072, People's Republic of China
E-mail: liangyan@nwpu.edu.cn

Abstract: Target tracking of over-the-horizon radar (OTHR) suffers from the effect of multi-path propagation. To date, all corresponding tracking methods depend on the precondition that the ionospheric heights should be available via the ionosondes. However, the ionosondes cannot be arbitrary deployed, for example, in sea area or hostile zone. This study presents the problem of sensor fusion of OTHR and a set of forward-based receivers (FBRs) for online mode identification of OTHR echoes, estimation of virtual ionospheric heights and localisation improvement. This fusion problem faces two challenges. The first is 'multi-path', as a kind of uncertainty existing in both the forward propagation of FBRs and the forward/backward propagation of OTHR. The other is 'coupling', representing the complexity that the mode/parameter identification and estimation couple each other. Here the joint optimisation scheme of identification and estimation is proposed mainly including four sub-processes: coordinate mapping with target height, joint identification and estimation of FBRs, mode identification of OTHR and localisation improvement. The simulation shows that propagation/clutter modes can be identified effectively and ionospheric heights are estimated without the help of ionosondes. Meanwhile, target state including the target height is estimated and the localisation accuracy is further improved due to sensor fusion.

1 Introduction

Over-the-horizon radars (OTHR) perform wide area surveillance by exploiting the refractive of high frequency (HF) propagation and track aircrafts, ballistic and cruise missiles, and ships beyond the line-of-sight horizon [1–4]. By the fact of its advantages, including long range (hundreds to thousands of kilometres) and wide surveillance area, OTHR is potentially powerful in surveillance missions.

Different from traditional radars, OTHR faces the challenge of multi-path propagation, whereby radar signals arrive at the receiver via different propagation paths and hence result in multiple echoes for one single target [5]. To date, there exist two kinds of approaches for OTHR target tracking. One utilises Kalman filters and data association in slant or radar coordinates, then involves in track fusion based on coordinate registration (CR), that is, the mapping between slant coordinates and ground coordinates [6, 7]. The other implements data association in slant coordinates and state estimate in ground coordinates and hence needs twice mapping between slant coordinates and ground coordinates. Its classical methods include multi-path data association (MPDA) [8, 9], probabilistic multiple hypothesis tracking (PMHT) [10, 11] and multi-path Viterbi data association [12, 13]. However, all the above methods have the same prerequisite that the virtual ionosphere heights (the key parameter in CR) should be detected by vertical and oblique ionosondes. As important components of OTHR systems, vertical and oblique ionosondes are utilised to detect the required ionospheric virtual heights [14, 15]. However, such virtual heights may be unavailable due to the constraints of deployment site, for example, in sea area or hostile zone.

Recently, much attention has been paid on introducing external sources of information, such as beacons or transponders [7, 16, 17], terrain features [17], additional OTHR systems [6] and passive receivers [18, 19]. The beacon-assisted method focuses on correcting the ground coordinates of each raymode by an amount determined from the radar signal transponded by a beacon. It is shown effective only within the neighbourhood of the beacon location. The terrain-assisted method is somewhat similar to the beacon-assisted method in principle and its uniqueness is to extract the correcting amount from prominent backscatter of geographical features. Owing to the large size of the resolution cell, the corresponding correction of the terrain-assisted method is rough. A set of azimuth-only sensors is introduced for OTHR [19] but limited by only improving the localisation accuracy on azimuth. The concept of a set of forward-based receivers (FBRs) augmented for OTHR is represented in [18]. However, the algorithm is not public. Besides, the radar tracks and the

precision navigation (PNAV) messages of large commercial airlines are attempted to be associated and the resultant reliable association is utilised to estimate the CR error for further refining the CR process [20].

Here, we present the problem of sensor fusion of OTHR and a set of FBRs for online propagation/clutter mode identification of OTHR echoes, estimation of virtual ionospheric heights and localisation improvement (including supplying the estimated target height). The considered problem triggers two challenges that have never been met before. The first is 'multi-path', as a kind of uncertainty exists in both the forward propagation of FBRs and the forward/backward propagation of OTHR. The other is 'coupling', representing the complexity that the mode/parameter identification and estimation couple each other (estimation errors increase identification risk while identification mistake leads to estimation divergence to the actual value). Here, a scheme of sensor fusion of OTHR and FBRs without the help of ionosondes is presented for joint mode identification and localisation. The scheme mainly includes four sub-processes: coordinate mapping with target height, joint identification and estimation of FBRs, mode identification of OTHR and localisation improvement. The simulation shows that the proposed method can effectively identify the propagation/clutter modes, and ionospheric heights can be estimated without the help of ionosondes. Meanwhile, target state including target height can be estimated and the localisation accuracy on azimuth and geographical distance from OTHR receiver to the target can be further improved through sensor fusion of OTHR and FBRs.

The rest of the paper is organised as follows: The problem is formulated in Section 2. Section 3 presents the scheme of mode identification and localisation improvement based on OTHR and FBRs. Section 4 presents simulations to evaluate and analyse the proposed scheme. Section 5 concludes the paper.

Throughout this paper, the superscripts 'i', 'l' and 'j' represent ith propagation mode for OTHR, lth forward propagation mode for FBR and jth FBR , respectively; the subscript 'k' represents kth time instant; the measurement sets of OTHR and FBRs are denoted by $Z_{1,k}$ and $Z_{2,k}$, respectively; the superscripts 't' and 'r' represent the propagation paths from the transmitter to the target and from the target to the receiver, respectively; L_1 and L_2 are the numbers of the possible virtual ionospheric refracting layers of backward and forward paths, respectively; N is the total number of FBRs.

2 Problem formulation

The scope of this paper is confined to localise a single target in a surveillance region of interest. For simplicity, we assume aircraft tracking under favourable ionospheric conditions that support single-hop propagation (reflection) via different ionospheric layers [5, 8]. Fig. 1 depicts the geometry of the target and radar sensor system including bistatic OTHR and FBRs, which is extended from the one neglecting target height in [5]. Note that the following assumptions for each OTHR/FBR echo at each time are satisfied: (i) Each ionosphere is to be associated with at most one measurement. (ii) Each measurement is to be associated with at most one ionosphere. The OTHR measurement model and FBRs measurement model are presented as follows.

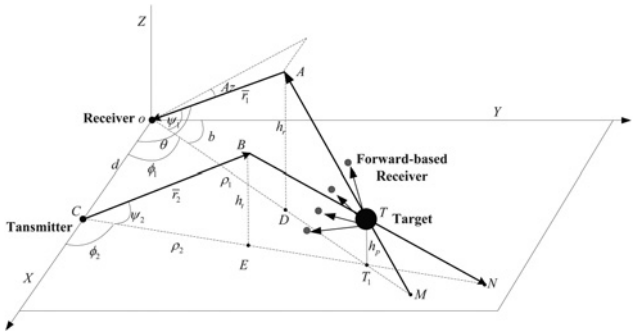

Fig. 1 *Geometry of OTHR and FBRs measurement model*

2.1 OTHR measurement model

Denote the target position at time instant k in the Cartesian coordinate system by $\tilde{X}_k = \mathrm{col}\{x_k, y_k, z_k\}$. Denote the measurement set of OTHR at time k by

$$Z_{1,k} = \{Z_{1,k}(1), Z_{1,k}(2), \ldots, Z_{1,k}(M_k)\} \tag{1}$$

where $Z_{1,k}(i) = \mathrm{col}\{\mathrm{Rg}_k(i), \mathrm{Az}_k(i)\}$, $i = 1, 2, \ldots, M_k$, with M_k being the total number of echoes at time instant k. The measurement of OTHR may originate from the interested target via one possible propagation path or just clutter. If $Z_{1,k}(i)$ comes from the interested target with the l_2^ith forward propagation and the l_1^ith backward propagation, then it can be modelled as follows

$$\begin{aligned} Z_{1,k}(i) &= H_1^{l_1^i, l_2^i}(\tilde{X}_k) + w_{1,k}(i) \\ &= \begin{bmatrix} \left(r_{1,k}^{l_1^i} + r_{2,k}^{l_2^i}\right)/2 \\ \sin^{-1}\left\{\sqrt{x_k^2 + y_k^2}\sin(b_k)/r_{1,k}^{l_1^i}\right\} \end{bmatrix} + w_{1,k}(i); \\ & l_1^i = 1, 2, \ldots, L_1,\ l_2^i = 1, 2, \ldots, L_2 \end{aligned} \tag{2}$$

where

$$r_{1,k}^{l_1^i} = \sqrt{\left(2h_k^{r,l_1^i} - z_k\right)^2 + x_k^2 + y_k^2} \tag{3}$$

$$r_{2,k}^{l_2^i} = \sqrt{\left(2h_k^{t,l_2^i} - z_k\right)^2 + (x_k - d)^2 + y_k^2} \tag{4}$$

$$b_k = \tan^{-1}(x_k/y_k) \tag{5}$$

and the measurement noise $w_{1,k}(i)$ is zero-mean and Gaussian with covariance $R_{1,k}(i) \triangleq \mathrm{cov}(w_{1,k}(i)) = \mathrm{diag}\{(\sigma_R)^2, (\sigma_A)^2\}$. Here h_k^{t,l_2^i} and h_k^{r,l_1^i} are the unknown virtual heights, respectively, representing the heights of the reflection points in forward path (from the transmitter to the target) and backward path (from the target to the receiver) related to $Z_{1,k}(i)$. As mentioned in [5], each propagation mode $\langle l_1^i, l_2^i \rangle$ produces an echo with a certain probability of detection. For simplicity, these detection probabilities are considered identical and denoted by P_D ($P_D \leq 1$).

It is widely accepted that clutter detections are independent from scan to scan, and the clutter (false measurement) model

is specified by a three-dimensional probability density function (pdf) $p_c(Z_{1,k}(i))$. The simplest and widely accepted clutter model is the uniform clutter pdf with a Poisson probability mass function for the total number of clutter measurements [5, 8]. If $Z_{1,k}(i)$ comes from the clutter, then its pdf satisfies

$$p_c(Z_{1,k}(i)) = \begin{cases} \dfrac{1}{V_G(k)}, & \text{if} \quad Z_{1,k}(i) \in G(k) \\ 0, & \text{otherwise} \end{cases} \tag{6}$$

Also, the probability mass function $g_c(n)$ for the number of clutter measurements being n within the validation region $G(k)$ is

$$p_c(Z_{1,k}(i)) = \begin{cases} \dfrac{1}{V_G(k)}, & \text{if} \quad Z_{1,k}(i) \in G(k) \\ 0, & \text{otherwise} \end{cases} \tag{7}$$

where λ_1 is chosen as N_k/V_s, with N_k the total number of detections in the scan and V_s the volume of the whole measurement space.

2.2 FBRs measurement model

Consider the case that the FBRs measure both azimuth and ground range, the measurement of the jth FBRs via the lth forward propagation at time k is

$$\begin{aligned} Z_{2,k}^{l,j} &= H_2^{l,j}(\tilde{X}_k) + w_{2,k}^j \\ &= \begin{bmatrix} \hat{H}_2^{l,j}(\tilde{X}_k) \\ \tan^{-1}\left(\dfrac{x_k - x_j}{y_k - y_j}\right) \end{bmatrix} + w_{2,k}^j, \\ & l = 1, 2, \ldots, L_2, \quad j = 1, 2, \ldots, N \end{aligned} \tag{8}$$

with

$$\begin{aligned} \hat{H}_2^{l,j}(\tilde{X}_k) = &\sqrt{\left(2h_k^{t,l} - z_k\right)^2 + (x_k - d)^2 + y_k{}^2} \\ &+ \sqrt{(x_k - x_j)^2 + (y_k - y_j)^2 + (z_k - z_j)^2} \end{aligned} \tag{9}$$

where $Z_{2,k}^{l,j} = \mathrm{col}\left\{z_{2,k}^{l,j}, b_k^j\right\}$ with $Z_{2,k}^{l,j}$ and b_k^j representing the range measurement and azimuth measurement of the jth FBR, respectively. (x_j, y_j, z_j) is the jth FBR coordinate in ground cartesian coordinates. The measurement noise $w_{2,k}^j$ is zero-mean and Gaussian with covariance $R_{2,k}^j \triangleq \mathrm{cov}(w_{2,k}^j) = \mathrm{diag}\left\{(\sigma_r)^2, (\sigma_b)^2\right\}$. The detection probability of FBRs is P_d. The clutter model is the same as that in OTHR measurement model with a different Poisson parameter λ_2.

The objective of this paper is to explore a scheme of sensor fusion of OTHR and FBRs without the help of ionosondes to jointly identify propagation modes and improve localisation accuracy as follows:

- Propagation/clutter modes of OTHR should be identified online. If mode identification can be effectively obtained, then the corresponding OTHR measurement model related to each echo will be appropriately chosen, which is the precondition for localisation improvement.
- Virtual ionospheric heights should be estimated. The virtual ionospheric heights, as the key environmental parameters of CR, affect the mode identification and localisation accuracy by the fact that the CR is essential in the OTHR-based tracking. If such height estimation is available, then it will be possible to propose the joint identification and estimation algorithm without the help of ionosondes.
- The target height should be estimated. The target height estimate is helpful to target discernment in situation assessment. Besides, the height estimate would be helpful in improving target localisation accuracy by the fact that ignoring the height will inevitably introduce localisation error.
- It is expected to achieve the improvement on the localisation accuracy through sensor fusion of OTHR and FBRs. The more accurate state estimate results in the smaller measurement validation region, which will reject more clutters. Meanwhile, the more accurate state estimate results in the sharper likelihood function, which is desirable in mode identification.

Remark 1: Traditionally, the target tracking problem of OTHR can be solved through the combination of Kalman filter and data association, given ionospheric heights and possible propagation modes detected by ionosondes. However, in this paper, the ionosondes are not always available, because of constraints of deployment site. Thus, introducing FBRs as external sources of information is expected to realise mode/parameter identification. Here mode identification and target localisation are deeply coupled and hence the joint identification and localisation is highly demanded.

Remark 2: Even if the ionosondes was available in neighbour interested zone, the obtained ionospheric data would still be not accurate because of spatial–temporal interpolation based on sparse sampling data [6, 14, 15]. It inevitably leads to errors in estimating ionospheric parameters and hence leads to systematic errors in the ground positions of targets. Hence, whether the ionosondes are available or not, it is highly demanded to explore the way of identifying ionospheric parameters without the help of ionosondes.

3 Mode identification and localisation improvement based on FBRs and OTHR

Considering the problem of joint estimation and identification, external sources of information, FBRs are augmented for OTHR. Utilising the additional information from FBRs, it is possible to estimate the ionospheric heights, identify the propagation modes and further improve the localisation accuracy, by the fact that the partial ionospheric parameters and target state are common in FBRs and OTHR. However, it brings a difficult problem about how to associate the data of OTHR and FBRs from different coordinates under the multi-path propagation.

doi: 10.1049/iet-rsn.2013.0017

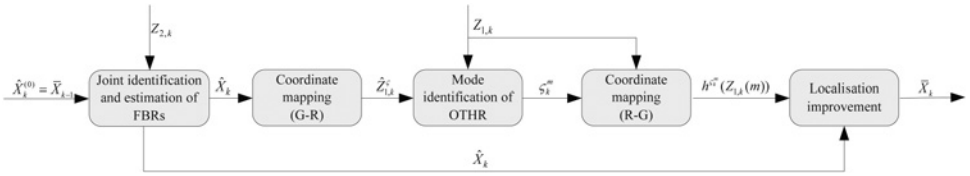

Fig. 2 *Flowchart of joint mode identification and localisation improvement scheme*

A framework of joint mode identification and localisation is proposed here and its flowchart is shown in Fig. 2, including the following modules:

- *Joint identification and estimation of FBRs:* It is needed to cluster FBRs range measurements with the same forward propagation for mode identification. And measurements of the optimal clustering solution are fused to obtain preliminary target state estimate of the common forward propagation and ionosphere heights estimate. Furthermore, the preliminary target state estimates related to different ionospheres are fused to obtain the final state estimate.
- *Coordinate mapping (G–R):* The final state estimate $\hat{X}_k$ is transformed from ground coordinates to radar coordinates, yielding measurement prediction $\hat{Z}_{1,k}^{\zeta}$ of different modes prepared for mode identification of OTHR measurements in radar coordinates.
- *Mode identification of OTHR:* A maximum-likelihood estimation-based data association rule between measurement prediction $\hat{Z}_{1,k}^{\zeta}$ of different modes and OTHR measurement $Z_{1,k}(m)$ is proposed to identify propagation mode ζ_k^m for the mth OTHR measurements.
- *Coordinate mapping (R–G):* The OTHR measurement $Z_{1,k}(m)$ of identified propagation mode ζ_k^m is transformed from radar coordinates to ground coordinates, yielding the corresponding state estimate $h^{\zeta_k^m}(Z_{1,k}(m))$ of OTHR measurement given specific propagation mode.
- *Localisation improvement:* Fuse state estimate $h^{\zeta_k^m}(Z_{1,k}(m))$ of OTHR measurement given specific propagation mode and the final state estimate $\hat{X}_k$ of FBRs in ground coordinates to improve the accuracy of target localisation in the minimum-variance sense.

It can be seen in Fig. 2 that twice coordinate mapping between radar coordinates and ground coordinates are needed in the flowchart. Hence, researching the coordinate mapping is helpful to reduce the systematic errors in the ground positions of target. The coordinate mapping (with target height) is first given as follows.

3.1 Coordinate mapping (with target height)

The estimate of target height is not only helpful in the improvement on the target localisation, but also desirable by target classification in situation awareness. However, for a bistatic OTHR, target height estimation was and is still a difficult problem. It is obvious that neglecting target height will inevitably cause system biases of mode identification and data association, thereby seriously restrict the performance of target tracking. In this paper, the mapping between radar coordinates and ground coordinates with target height is derived to provide the possibility of estimating the target height. ch relied heavily on the dwell-to-dwell variations, the coherent integration time, radar bandwidth and observation time. The method proposed in this paper is much more feasible, which estimates the target height via data fusion rather than signal processing.

As shown in Fig. 1, the OTHR receiver is at the origin, with the transmitter situated at distance d from it. Projections on the X–Y plane of range from the target to the receiver and from the transmitter to the target are ρ_1 and ρ_2, respectively. Elevations are ψ_1 and ψ_2, respectively. Azimuths are ϕ_1 and ϕ_2, respectively. The ray paths from the transmitter to the target and from the target to the receiver are assumed to be reflected from idealised ionospheric layers at virtual heights h_t and h_r, respectively. The state variables in ground coordinates for the interested target, are the ground range $\rho \triangleq \sqrt{{\rho_1}^2 + z^2}$, range rate $\dot{\rho}$, bearing with respect to bore sight $b \triangleq \pi/2 - \phi_1$, with $\phi_1 = \angle\mathrm{DOC}$ and azimuth rate $\dot{b}$. As illustrated in [5], azimuth rate remains small due to the large range, thus may be taken zero. The target height is $z = \overline{TT}_1$. OTHR measurements are path length $\mathrm{Rg} \triangleq (\bar{r}_1 - \overline{TM}/2) + (\bar{r}_2 - \overline{TN}/2)$, with $\bar{r}_1 = \overline{OA}$, $\bar{r}_2 = \overline{CB}$, azimuth $Az = \pi/2 - \theta$, with $\theta = \angle\mathrm{AOX}$ and Doppler $\mathrm{Rr} \triangleq \mathrm{Rg}$. The following theorem is presented to establish the mapping between radar coordinates and ground coordinates.

Theorem 1: The mapping from ground coordinates (ρ, $\dot{\rho}$, b) to radar coordinates (Rg, Rr, Az) is (see (10))

with

$$r_1 = \sqrt{(2h_r - z)^2 + \rho^2 - z^2} \tag{11}$$

$$r_2 = \sqrt{(2h_t - z)^2 + d^2 + \rho^2 - 2d\sqrt{\rho^2 - z^2}\sin b - z^2} \tag{12}$$

$$\begin{cases} \mathrm{Rg} = (r_1 + r_2)/2 \\ \mathrm{Rr} = (\rho\dot{\rho} - 2h_r\dot{z})/(2r_1) + (\rho\dot{\rho} - 2h_t\dot{z})/(2r_2) - (x\dot{x} + y\dot{y})d\sin(b)/\left(2r_2\sqrt{\rho^2 - z^2}\right) \\ \mathrm{Az} = \sin^{-1}\left[\sqrt{\rho^2 - z^2}\sin(b)/r_1\right] \end{cases} \tag{10}$$

The inverse mapping from radar coordinates to ground coordinates is (see (13))

with

$$r_1 = \frac{4\mathrm{Rg}^2 - (2h_t - z)^2 - d^2 + (2h_r - z)^2}{4\mathrm{Rg} - 2d\sin(\mathrm{Az})} \tag{14}$$

$$r_2 = 2\mathrm{Rg} - r_1 \tag{15}$$

Remark 3: Theorem 1 provides a more general mapping between radar and ground coordinates. It is obvious that our proposed coordinate mappings in (10)–(15) take the model [5, 8] as the special case that the target height above sea level equals zero.

Remark 4: Deriving the mapping with target height between radar coordinates and ground coordinates has multiple advantages. First, it establishes the relationship between target height and OTHR measurement, and hence provides the possibility to estimate the target height. Second, through considering the target height, the target localisation model is more accurate by the fact that the zero-valued height approximation utilised in the previous mapping [5, 8] inevitably introduces the localisation error in the X–Y plane.

3.2 Joint identification and estimation of FBRs

By the fact that FBRs can receive the range measurements from all the ionospheres, which results in the problems of forward multi-path propagation uncertainty of FBRs, it is essential to consider the problem of clustering all FBR measurements with the same forward propagation. It is possible to obtain the ionospheric parameters and rough target state estimate via fusing a set of FBRs, by the fact that only forward propagation uncertainty exists in the FBR measurements.

3.2.1 Mode identification: In this section, FBRs mode identification is implemented through minimising the optimal clustering function with two parts, generalised likelihood ratios and homologous mode statistic. The generalised likelihood ratios as assignment costs for the candidate associations are widely applied in the general S-tuple dimension assignment [21, 22], which are globally minimised to determine the optimal S-tuple measurements with the same origin. Also, the homologous mode statistic for mode identification draws inspiration from the track-to-track correlation algorithms [23–25], in which two estimates from different tracks are utilised to test the hypothesis that these estimates are from the same target. The corresponding relationships between the track-to-track correlation and the homologous mode statistic for mode identification are given in Table 1. Given hypothesis of assigning measurements to the specific modes, mode-conditional state estimates are hence obtained. Based on our proposed homologous mode statistic measuring the difference between the mode-conditional state estimates, the association hypothesis is scored. If the difference between the mode-conditional state estimates is minor, the association hypothesis will be accepted. Another possible method to solve FBRs mode identification is to utilise the generalised likelihood ratio merely. However, such method only measures the difference between the measurements and the mode-conditional predicted measurements. It is expected that introducing the homologous mode statistic will bring out the further improvement on mode identification, by the fact that the measurements difference together with the mode-conditional state estimates difference are both utilised.

Table 1 Corresponding relationships between the track-to-track correlation and the homologous mode statistic

Algorithms	Track-to-track correlation	Homologous mode statistic
object	decide whether the tracks are from the same target	decide whether the mode-conditional state estimates are for the same target
input	estimates of different tracks	estimates related to different modes
criterion	if the difference between state estimates is less, it is more likely the tracks are from the same target	if the difference between mode-conditional state estimates is less, it is more likely the association hypothesis is acceptable

Denote the range measurements set of jth FBR with unknown propagation mode at time k as $z_{2,k}^{j} = \left\{z_{2,k}^{1,j}, z_{2,k}^{2,j}, \ldots, z_{2,k}^{m(k,j),j}\right\}$ with $m(k, j)$ being the total number of range measurements of jth FBR at time k. Create association hypothesis that range measurements set $\left\{z_{2,k}^{i_1,1}, z_{2,k}^{i_2,2}, \ldots, z_{2,k}^{i_j,j}, \ldots, z_{2,k}^{i_N,N}\right\}$ stem from the same lth forward propagation with i_j representing the serial number in the range measurements set of jth FBR. Denote the above N-tuple of range measurements by $z_{i_1,i_2,\ldots,i_N}^{l} = \left\{z_{2,k}^{i_1,1}, z_{2,k}^{i_2,2}, \ldots, z_{2,k}^{i_N,N}\right\}$, whose measurement noises are mutually independent.

Generalised likelihood ratio: The event that the range measurement set $z_{i_1,i_2,\ldots,i_N}^{l}$ originates from the interested target via the common lth forward propagation or spurious sources are denoted by E and Φ, respectively. The corresponding likelihood functions are

$$r_2 = 2\mathrm{Rg} - r_1 \tag{16}$$

$$\Lambda\left(z_{i_1,i_2,\ldots,i_N}^{l} \middle| \Phi\right) = \prod_{j=1}^{N} [1/\Psi]^{u(i_j)} \tag{17}$$

where Ψ is the validation region of FBRs and $u(i_j)$ is the

$$\begin{cases} \rho = \sqrt{z^2 + r_1^2 - (2h_r - z)^2} \\ \dot{\rho} = \left[2\mathrm{Rr} + 2\left(\dfrac{h_r}{r_1} + \dfrac{h_t}{r_2} - \dfrac{z}{2r_2} \cdot \dfrac{d\sin b}{\sqrt{\rho^2 - z^2}}\right)\dot{z}\right]\left[\dfrac{\rho}{r_1} + \dfrac{\rho}{r_2}\left(1 - \dfrac{d\sin b}{\sqrt{\rho^2 - z^2}}\right)\right] \\ b = \sin^{-1}\left[r_1 \sin(\mathrm{Az})/\sqrt{\rho^2 - z^2}\right] \end{cases} \tag{13}$$

doi: 10.1049/iet-rsn.2013.0017

Kronecker delta function defined by

$$u(i_j)=\begin{cases}0, & \text{if } z_{2,k}^{i_j,j} \text{ is out of the prediction door}\\ 1, & \text{otherwise}\end{cases} \tag{18}$$

Thus, the generalised likelihood ratio is given by

$$\begin{aligned}c_{i_1,i_2,\cdots,i_N}^{l}&=-\ln\frac{\Lambda\left(z_{i_1,i_2,\ldots,i_N}^{l}\middle|E\right)}{\Lambda\left(z_{i_1,i_2,\ldots,i_N}^{l}\middle|\Phi\right)}\\&=\sum_{j=1}^{N}\left\{\left[u(i_j)-1\right]\ln\left(1-P_d\right)\right.\\&\quad-u(i_j)\ln\left(\frac{P_d\Psi}{|2\pi R|^{1/2}}\right)+\frac{u(i_j)}{2}\\&\quad\left.\left[z_{2,k}^{i_j,j}-\hat{H}_2^{l,j}\left(\hat{X}_{k-1}\right)^{T}R^{-1}\left[z_{2,k}^{i_j,j}-\hat{H}_2^{l,j}(\hat{X}_{k-1})\right]\right]\right\}\end{aligned} \tag{19}$$

where $\hat{X}_{k-1}$ is the final target state estimate fusing state estimates related to different ionospheres based on the minimum variance estimation rule calculated via (21) at time $k-1$, and $\hat{H}_2^{l,j}$ is defined in (9).

Homologous mode statistic: To further improve the performance of FBRs mode identification, introduce the context information to the optimal clustering function, that is, the state estimate and corresponding covariance related to the lth forward propagation. Utilising the state estimates of all forward propagations except the L_2th to predict the state estimate of the L_2th forward propagation and construct the following hypothesis testing statistic Γ representing the homologous mode. Since the estimate error of target state from arbitrary two models are independent, the error is zero-mean and Gaussian distributed

$$\Gamma=\hat{X}_k^{L_2}-\frac{1}{L_2-1}\sum_{l=1}^{L_2-1}\hat{X}_k^{l} \tag{20}$$

$$\Gamma\sim N\left(0,P_{2,k}^{L_2}+\frac{1}{(L_2-1)^2}\sum_{l=1}^{L_2-1}P_{2,k}^{l}\right) \tag{21}$$

The logarithmic probability density function of homologous mode statistic Γ is given below

$$\begin{aligned}L_{z^1,z^2,\ldots,z^{L_2}}&=-\ln 2\pi-\frac{1}{2}\ln\left(P_{2,k}^{L_2}+\frac{\sum_{l=1}^{L_2-1}P_{2,k}^{l}}{(L_2-1)^2}\right)\\&\quad-\frac{1}{2}\Gamma^{\mathrm{T}}\left(P_{2,k}^{L_2}+\frac{\sum_{l=1}^{L_2-1}P_{2,k}^{l}}{(L_2-1)^2}\right)^{-1}\Gamma\end{aligned} \tag{22}$$

where $\hat{X}_k^{l}$ and $P_{2,k}^{l}$ are, respectively, obtained in (12) through several iterations and (20) via non-linear fitting the measurements originating from the same ionosphere l introduced in the next section.

To illustrate the homologous mode more clearly, consider the case where two forward propagation modes E and F exist (i.e. $L_2=2$). If the difference between the mode-conditional state estimate $\hat{X}_k^{E}$ through fusing measurements $z_{1,1,1,1}^{E}$ and state estimate $\hat{X}_k^{F}$ through fusing measurements $z_{2,2,2,2}^{F}$ is not distinct, then the association hypothesis will be accepted that the range measurement sets $\left\{z_{2,k}^{1,1},z_{2,k}^{1,2},z_{2,k}^{1,3},z_{2,k}^{1,4}\right\}$ and $\left\{z_{2,k}^{2,1},z_{2,k}^{2,2},z_{2,k}^{2,3},z_{2,k}^{2,4}\right\}$ originate from E layer and F layer, respectively. The advantages of utilising homologous mode in the mode identification are shown as follows. First, here eight measurements are utilised to support the hypothesis simultaneously, instead of only four measurements in the general S-tuple dimension assignment. In other words, compared with the generalised likelihood ratios, introducing homologous mode brings out the joint association scheme based on multiple homologous measurements. By the fact that more measurements always have more information, which will definitely decrease the uncertainty and hence improve the association quality. Secondly, it is widely accepted that the state estimate after appropriate filtering is much closer to the true value compared with the measurement value [26]. Thus introducing the homologous mode statistic representing the difference between the mode-conditional state estimates is hopeful to implement FBRs mode identification more effectively, compared with the generalised likelihood ratios which only measures the difference between the measurements and the mode-conditional predicted measurements.

Combining the logarithmic probability density function in (22) and the generalised likelihood ratio in (19), we can obtain the optimal clustering solution of FBR measurements with the common forward propagation as follows

$$C_l^{*}=\arg\min_{i_1,i_2,\ldots,i_N}\left\{\frac{\sum_{l=1}^{L_2}c_{i_1,i_2,\ldots,i_N}^{l}}{L_{z^1,z^2,\ldots,z^{L_2}}}\right\} \tag{23}$$

Remark 5: The almost all OTHR tracking methods, for example in [5, 8], consider the most common situation that there only exist two ionospheric layers (E and F) with four one-hop propagation modes: EE, EF, FE and FF, that is, $L_2=2$. In such situation, the number of association hypotheses is $L_2^{N-1}=8$ with $N=4$ representing the number of FBR. It is not too complex and hence can be solved by the exhaustive method. Of course, a more realistic ionospheric model may characterise more virtual ionospheric layers. For example, the F layer could split into upper and lower layers $F1$ and $F2$, or a sporadic E layer might be formed. In such a case, the dimension of the optimisation presented above would be large and hence the biologically-inspired optimisation method would be suitable; for example, ant-colony method [27, 28], neural network method [29], genetic method [30] and the infectious disease model [31].

3.2.2 State estimate: Given the optimal clustering solution C_l^{*}, the FBR measurement set $Z_{2,k}=\left\{Z_{2,k}^{i_1^{*},1},Z_{2,k}^{i_2^{*},2},\ldots,Z_{2,k}^{i_N^{*},N}\right\}$ originating from the lth forward propagation are fused to obtain the preliminary state estimate of lth forward propagation via the non-linear fitting method. Augment the state vector as $X_k^{l}=\mathrm{col}\left\{x_k^{l},y_k^{l},z_k^{l},h_k^{l}\right\}$, where h_k^{l} denotes the ionosphere height of lth forward propagation. The dath iteration estimate of lth forward propagation at time k is given by

$$\begin{aligned}\hat{X}_k^{\lambda,l}&=\hat{X}_k^{\lambda-1,l}+\left(\left(J_{2,k}^{\lambda-1,l}\right)^{\mathrm{T}}R^{-1}J_{2,k}^{\lambda-1,l}\right)^{-1}\left(J_{2,k}^{\lambda-1,l}\right)^{\mathrm{T}}\\&\quad\times R^{-1}\left(Z_{2,k}-H_2\left(\hat{X}_k^{\lambda-1,l}\right)\right)\end{aligned} \tag{24}$$

where initial iteration value at time k is the fusion estimate of time $k-1$, that is, $\hat{X}_k^{0,l} = \bar{X}_{k-1}$, which is calculated in Section 3.4

$$R = \text{diag}\{R_2^j\}, j = 1, 2, \ldots, N \tag{25}$$

$$H_2\left(\hat{X}_k^{\lambda-1,l}\right) = \left[H_{2,1}\left(\hat{X}_k^{\lambda-1,l}\right); \quad H_{2,2}\left(\hat{X}_k^{\lambda-1,l}\right), \ldots, H_{2,N}\left(\hat{X}_k^{\lambda-1,l}\right)\right] \tag{26}$$

$$H_{2,j}\left(\hat{X}_k^{\lambda-1,l}\right) = \left[\begin{array}{c} \Upsilon(1) + \Upsilon(2) \\ \tan^{-1}\left(\dfrac{\hat{x}_k - x_j}{\hat{y}_k - y_j}\right) \end{array}\right]_{\hat{X}_k = \hat{X}_k^{\lambda-1,l}} \tag{27}$$

$$j = 1, 2, \ldots, N$$

$$J_{2,k}^{\lambda-1,l} = [J_{2,k}^{1,\lambda-1}, J_{2,k}^{2,\lambda-1}, \ldots, J_{2,k}^{N,\lambda-1}] \tag{28}$$

(see (29))

$$\Upsilon(1) = \sqrt{\left(2\hat{h}_k - \hat{z}_k\right)^2 + (\hat{x}_k - d)^2 + \hat{y}_k{}^2} \tag{30}$$

$$\Upsilon(2) = \sqrt{(\hat{x}_k - x_j)^2 + (\hat{y}_k - y_j)^2 + (\hat{z}_k - z_j)^2} \tag{31}$$

The iteration will stop if $\left(\left\|\hat{X}_k^{\lambda+1,l} - \hat{X}_k^{\lambda,l}\right\| / \left\|\hat{X}_k^{\lambda,l}\right\|\right) < \tau$, with $0 < \tau < 1$, or the number of iteration reaches a pre-specified upper bound ε. At every iteration l at time k, the Jacobin matrix is calculated iteratively. By the fact that $J_{2,k}^{\lambda-1,l}$ is a full column rank and R is a positive definite, the matrix $\left(J_{2,k}^{\lambda-1,l}\right)^{\mathrm{T}} R^{-1} J_{2,k}^{\lambda-1,l}$ is always full rank, and hence guarantees the solution uniqueness, that is, the location estimate will converge to the optimum solution from reasonable initialisations [26]. The covariances of state estimate error related to the lth forward propagation in ground coordinates is given

$$\begin{aligned} P_{2,k}^l &= E\left(\left(\hat{X}_k - X_k\right)\left(\hat{X}_k - X_k\right)^{\mathrm{T}}\right) \\ &= \left(\left(J_{2,k}^{\lambda-1}\right)^{\mathrm{T}} R^{-1} J_{2,k}^{\lambda-1}\right)^{-1} \end{aligned} \tag{32}$$

Furthermore, the target state estimates related to different ionospheres, $\left\{\hat{X}_k^1, \hat{X}_k^2, \ldots, \hat{X}_k^{L_2}\right\}$ are fused via the minimum variance estimation rule to obtain the final target state estimate, given by

$$\hat{X}_k = P_{2,k}\left(\sum_{l=1}^{L_2} \left(P_{2,k}^l\right)^{-1} \hat{X}_k^l\right) \tag{33}$$

$$P_{2,k} = \left(\sum_{l=1}^{L_2} \left(P_{2,k}^l\right)^{-1}\right)^{-1} \tag{34}$$

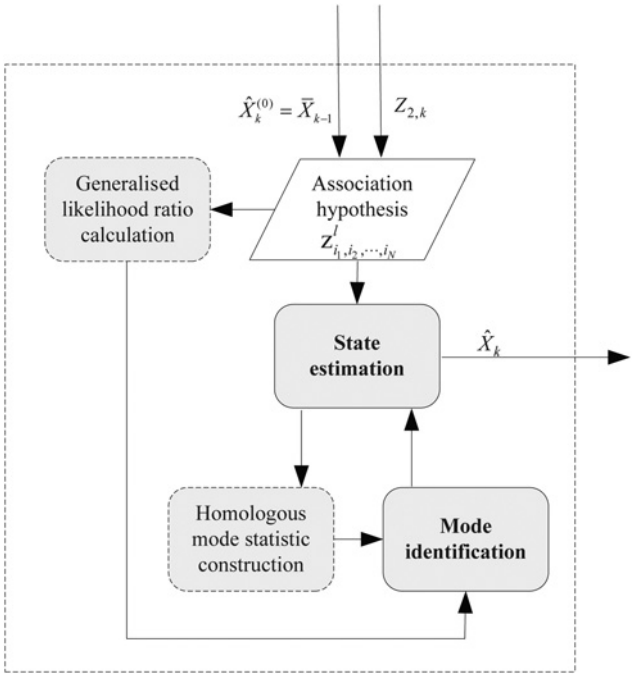

Fig. 3 *Functional flow of joint identification and estimation of FBRs*

The implementation of joint identification and estimation of FBRs is shown in Fig. 3. First, give an N-tuple of range measurements, hypothesising that the range measurement set stems from the same forward propagation. Then, calculate the generalised likelihood ratio that the N-tuple of range measurements originate from the same forward propagation by (19). Next, construct the homologous mode statistic by (20) utilising the preliminary state estimates related to different forward propagations defined in (24). After that, obtain the optimal clustering solution of FBRs measurements by (23) with the common forward propagation mode based on the generalised likelihood ratio and the logarithmic probability density function defined in (22) in the maximum-likelihood sense. Finally, target state estimates related to different ionospheres are fused to obtain the final target state by (33).

3.3 Mode identification of OTHR

The preliminary state estimate $\hat{X}_k$ obtained from the above section is transformed from ground coordinates into radar coordinates, yielding the corresponding measurement prediction value $\hat{Z}_{1,k}^{\zeta} = H_1^{\zeta}(\hat{X}_k)$. The error vector for the mth OTHR measurement corresponding to l_1th backward propagation and l_2th forward propagation and clutter mode is given by

$$\Delta_k^{\zeta}(m) = \left[\begin{array}{c} \mathrm{Rg}_k^m - \mathrm{Rg}_k^{\zeta} \\ \mathrm{Az}_k^m - \mathrm{Az}_k^{\zeta} \end{array}\right]; \quad \zeta \in \{\langle l_1, l_2\rangle \cup 0\}, \quad m \in \{0, 1, \ldots, M_k\} \tag{35}$$

$$J_{2,k}^{j,\lambda-1} = \left[\begin{array}{cccc} \dfrac{x - x_j}{\Upsilon(1)} + \dfrac{x - d}{\Upsilon(2)} & \dfrac{y - y_j}{\Upsilon(1)} + \dfrac{y}{\Upsilon(2)} & \dfrac{z - z_j}{\Upsilon(1)} + \dfrac{2h_i - z}{\Upsilon(2)} & \dfrac{4h_i - 2z}{\Upsilon(2)} \\ \dfrac{y - y_j}{(x - x_j)^2} + (y - y_j)^2 & \dfrac{x_j - x}{(x - x_j)^2} + (y - y_j)^2 & 0 & 0 \end{array}\right]\Bigg|_{\hat{X}_k = \hat{X}_k^{\lambda-1,l}} \tag{29}$$

$$i = 1, 2, \cdots, L_2 \; j = 1, 2, \cdots, N$$

doi: 10.1049/iet-rsn.2013.0017

Also, the likelihood function identifying propagation/clutter modes of the mth measurement is given by (see (36))

where $\zeta = 0$ denotes clutter mode, and $P_k^{\zeta}(m) = P_{1,k}^{\zeta}(m) + P_{2,k}P_{1,k}^{\zeta}(m) \triangleq E\left(\left(Z_{1,k}(m) - H_1^{\zeta}(\hat{X}_k)\right)\left(Z_{1,k}(m) - H_1^{\zeta}(\hat{X}_k)\right)^{\mathrm{T}}\right)$.

Based on the above likelihood function, a maximum-likelihood estimation-based data association rule is proposed to identify the propagation modes ζ_k^m of OTHR measurement $Z_{1,k}(m)$ at time k as follows

$$\zeta_k^m = \arg \max_{\zeta \in \{\langle l_1, l_2 \rangle \cup 0\}} \{LF_k(m)\} \tag{37}$$

Thus, the measurement $Z_{1,k}(m)$ of OTHR echoes at time k is hence related to propagation modes ζ_k^m.

3.4 Localisation improvement

A minimum variance estimation method is given to improve the accuracy of target localisation by fusing state estimate of OTHR measurement given specific propagation mode and preliminary state estimate of FBRs in ground coordinates. Since the measurement noises from OTHR and FBRs are independent, the optimal fusion is the linear weighted function of the two estimates. The estimate fusion has the following expression

$$\bar{X}_k = \sum_{m=1}^{M_k} \sum_{\zeta_k^m \neq 0} c_m \left[h^{\zeta_k^m}\left(Z_{1,k}(m)\right)\right] + c_0 \hat{X}_k \tag{38}$$

subject to the following constraint

$$\sum_{m=1}^{M_k} \sum_{\zeta_k^m \neq 0} c_m + c_0 = 1 \tag{39}$$

where $h^{\zeta_k^m}\left(Z_{1,k}(m)\right)$ denotes state estimate of OTHR measurement $Z_{1,k}(m)$ transformation from radar coordinates into ground coordinates via propagation mode ζ_k^m. Through simple derivation, the optimal parameters are obtained as follows

$$c_m^{\mathrm{opt}} = \left(P_{1,k}^{\zeta_k^m}(m)\right)^{-1} \left(\sum_{m=1}^{M_k} \sum_{\zeta_k^m \neq 0} \left(P_{1,k}^{\zeta_k^m}(m)\right)^{-1} + (P_{2,k})^{-1} \right)^{-1} \tag{40}$$

$$c_0^{\mathrm{opt}} = (P_{2,k})^{-1} \left(\sum_{m=1}^{M_k} \sum_{\zeta_k^m \neq 0} \left(P_{1,k}^{\zeta_k^m}(m)\right)^{-1} + (P_{2,k})^{-1} \right)^{-1} \tag{41}$$

Based on the four sections, the calculation steps of the proposed scheme is shown in Table 2.

Table 2 Calculation steps of the proposed scheme

Initialisation ($k = 0$): $\hat{X}_0^{(0)} = X_0$

for $k = 1{:}T$, $\hat{X}_k^{(0)} = \bar{X}_{k-1}$

1. Calculate the generalised likelihood ratio and the logarithmic probability density function of homologous mode statistic Γ, by (19) and (22)
2. Obtain the optimal clustering solution of FBR measurements with common forward propagation by (23). Fuse the measurements of optimal clustering solution to obtain the preliminary state estimate of lth forward propagation, by (24)
3. Fuse the state estimates related to different ionospheres to obtain the final target state estimate $\hat{X}_k$ and the corresponding covariance $P_{2,k}$ by (33) and (34), respectively
4. Transform the above $\hat{X}_k$ from ground coordinates to radar coordinates by (10) via $L_1L_2 + 1$ propagation modes, yielding the corresponding measurement prediction value $\hat{Z}_{1,k}^{\zeta}$
5. Identify the propagation modes ζ_k^m of OTHR measurement $Z_{1,k}(m)$ by (37)
6. Transform OTHR measurement $Z_{1,k}(m)$ from radar coordinates to ground coordinates via propagation mode ζ_k^m by (13) to obtain the state estimate of OTHR measurement, and fuse the result with $\hat{X}_k$ in Step 3 by (4). The fused state $\bar{X}_k$ is the initial iteration value at time $k+1$

4 Simulation results

Considering the surveillance area with distance from 800 to 1300 km, and azimuth from 0.06981 to 0.17453 rad, the distance between the OTHR receiver and transmitter is 200 km. The four FBRs are located at positions (573.58 km 819.15 km, 0), (642.79 km, 766.04 km, 0), (766.04 km, 642.79 km, 0) and (819.15 km, 573.58 km, 0), respectively. Consider a single target moves at a constant velocity in the ground coordinates, with initial position (1060.66 km, 1060.66 km, 30 km) and velocity (0.25 km/s, 0.25 km/s,0). The sampling interval is 10 s, and the total simulation step is 100. The standard covariances of OTHR measurement noises are $\sigma_R = 5$ km and $\sigma_A = 0.003$ rad, respectively. The standard covariances of FBRs measurement noises are $\sigma_r = 1$ km and $\sigma_b = 0.002$ rad, respectively. Because of the scope of the present paper limited to target localisation, the Doppler measurements of target are not utilised. Here, we consider the case of two virtual ionospheric layers and accordingly each target produces up to four echoes. The simulation parameters for FBRs are ($P_d = 0.9$, $\lambda V = 200$), and the ideal assumption for FBRs ($P_d = 1$, $\lambda V = 0$) is considered for comparison in the following sections. In fact the measurements of FBRs are obtained via single ionospheric refraction compared with double refractions of OTHR. Moreover, the strength of signals is inversely proportional to the distance to the fourth power ($1/R^4$), thus the signal strength of OTHR is much lower than that of FBRs, being 1/16 of the FBRs signal strength. Therefore the signal strength of FBRs would be powerful enough and hence the ideal case of $P_d = 1$ and $P_f = 0$ is considered here. Such cases represent somewhat the upper-bound performance.

Here, three simulation cases are given for method verification. In the first case about target localisation, target states including the target height and ionospheric heights

$$\mathrm{LF}_k(m) = \begin{cases} \dfrac{1}{2\pi \left|P_k^{\zeta}(m)\right|^{1/2}} \exp\left\{-\dfrac{1}{2}\left(\Delta_k^{\zeta}(m)\right)^{\mathrm{T}} \left(P_k^{\zeta}(m)\right)^{-1} \Delta_k^{\zeta}(m)\right\}; & \text{for} \quad \zeta = \langle l_1, l_2 \rangle \\ \lambda \sqrt{\det\left(2\pi P_k^{\zeta}(m)\right)} \dfrac{1 - P_D P_G}{P_D}; & \text{for} \quad \zeta = 0 \end{cases} \tag{36}$$

are estimated under different probabilities of detection and false alarm for FBRs. Besides, the statistical results for FBRs mode identification with and without the homologous mode statistic are performed. In the second case, propagations/clutter modes of OTHR measurements are identified to verify the accuracy of the maximum-likelihood-estimation based data association. In the last case, based on the above mode identification results, information of OTHR and FBRs are fused to further improve the localisation accuracy. Note that the proposed method in this paper mainly aims at estimating target height and ionospheric heights, and realising the joint identification and localisation improvement. Unfortunately, the algorithms mentioned in [6, 7, 16–20] are not suitable to solve the proposed problem. Hence, in the following simulation cases, method comparison is not considered.

4.1 Target localisation

Consider that the ray paths are reflected from idealised ionospheric layers E and F. Table 3 shows the statistical results of FBRs mode identification with and without the homologous mode statistic. It can be seen that the introduced homologous mode statistic improves the performance in FBRs mode identification.

The preliminary target state estimate error in x/y-axis, target height estimate and E/F ionosphere height estimate are given in Figs. 4–6 compared with the ideal assumption scenario. It is seen that the target height and two ionosphere heights are effectively estimated. Also, it is shown that the performance of estimation of target state and ionospheric heights only decreases slightly compared with the ideal assumption, which reflects the forward propagation mode for FBRs is well identified. The estimate of target height estimate is helpful to target discernment desirable in situation assessment. The estimate of target height and ionosphere heights seem rougher than that of positions in x-axis and y-axis, reflecting the fact that the height estimation is harder.

Table 3 Statistical results of FBRs mode identification

	($P_d = 0.9$, $\lambda V = 200$) with homologous mode statistic, %	($P_d = 0.9$, $\lambda V = 200$) without homologous mode statistic, %
layer *E*	83	74
layer *F*	75	64

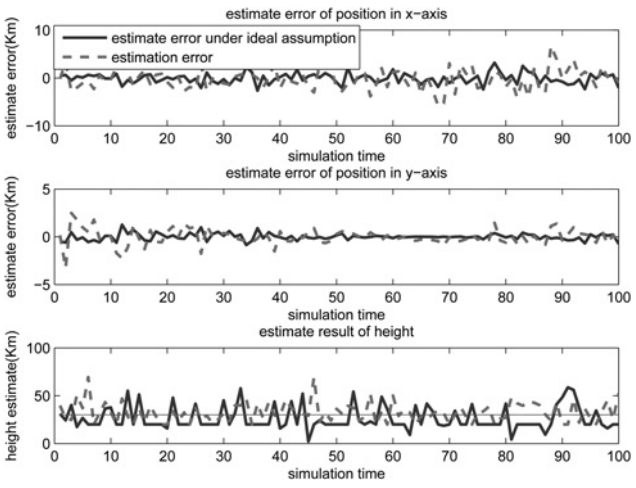

Fig. 4 *Estimate error of preliminary target state*

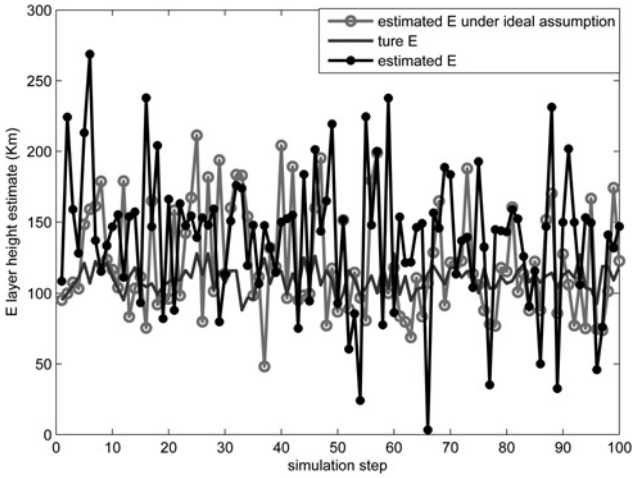

Fig. 5 *Estimate of ionosphere E height*

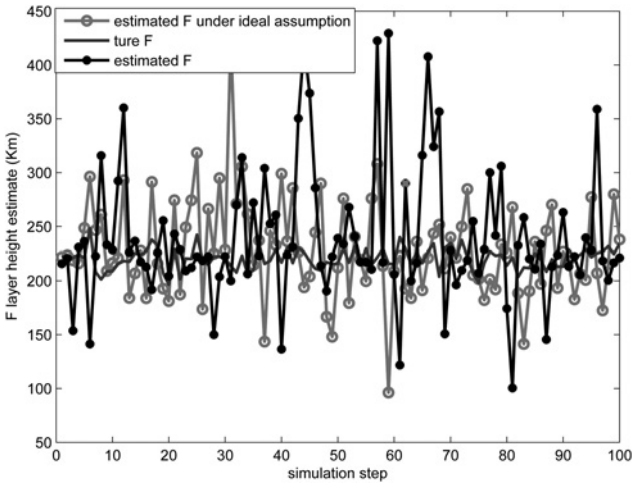

Fig. 6 *Estimate of ionosphere F height*

4.2 Mode identification

Table 4 shows the mode identification rate of OTHR measurements based on four FBRs under the ideal assumption for FBRs. Although Table 5 shows the results under the simulation parameters of $P_d = 0.9$, $\lambda V = 200$ for FBRs, in which P_{ij} denotes the statistical probability of mode i identified as mode j, and $i = 0$ denotes clutter mode.

Table 4 Statistical results of mode identification ($p_d = 1$, $\lambda V = 0$)

i	0	1	2	3	4
			J		
0	**84.65**	4.62	4.02	3.59	3.12
1	3.84	**78.44**	4.22	7.48	6.02
2	4.54	7.12	**65.34**	4.15	18.85
3	2.68	7.04	4.03	**67.29**	18.96
4	3.56	0.89	12.33	4.88	**78.34**

doi: 10.1049/iet-rsn.2013.0017

Table 5 Statistical results of mode identification ($p_d = 0.9$, $\lambda V = 200$)

i/*j*	0	1	2	3	4
0	**84.46**	3.62	4.26	3.22	4.44
1	4.09	**69.03**	4.04	8.93	13.91
2	3.8	7.51	**59.63**	24.6	4.46
3	4.24	8.86	16.2	**61.23**	9.47
4	4.79	20.16	3.71	4.23	**67.11**

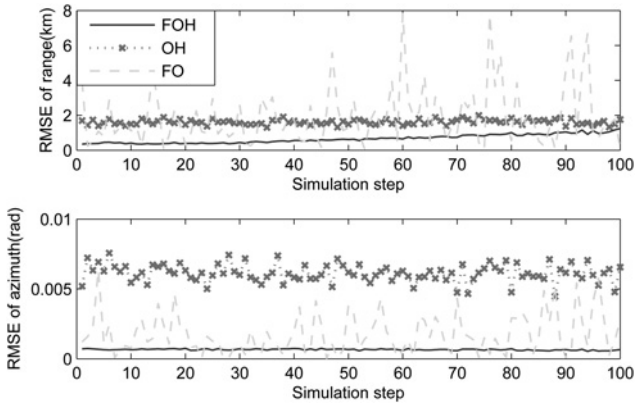

Fig. 7 *RMSE of target localisation comparison*

It can be seen from Tables 4 and 5 that the proposed method can effectively identify the propagation/clutter modes through the bold number in diagonal line, which shows that the each propagation/clutter mode is mostly successfully identified. Besides, it is found that the mode identification rates of mode 1(EE) and mode 4(FF) are relatively higher than that of mode 2(EF) and mode 3(FE), which coincides with the outstanding range measurements of mode 1(EE) and mode 4(FF). Also, it is shown that the statistical results of OTHR mode identification only reduce little compared with the ideal assumption, which coincides with the results shown in Figs. 4–6.

4.3 Target localisation improvement

Based on the above mode identification results, Fig. 7 shows the root-mean-square error (RMSE) of target localisation comparison of three different settings: four FBRs augmented for OTHR considering target height (FOH), only OTHR considering target height (OH) and four FBRs augmented for OTHR neglecting target height (FO) based on 100 Monte-Carlo runs. It can be seen that the proposed scheme improves target localisation accuracy both on azimuth and geographical distance from OTHR receiver to the target considering target height and introducing FBRs. And neglecting target height significantly decreases the localised accuracy.

5 Conclusion

This paper proposes a scheme of sensor fusion of OTHR and FBRs to realise the joint mode identification and target localisation. The mapping between radar coordinates and ground coordinates is derived. In mode identification, propagation modes and ionospheric heights as environmental parameters are identified online without the help of ionosondes, respectively. In target localisation, target state can be estimated including the target height, which is helpful to target discernment desirable in situation assessment. Besides, the localisation accuracy through fusing information from OTHR and FBRs is further improved on azimuth and geographical distance from OTHR receiver to the target.

6 Acknowledgment

This work was supported by the National Science Foundation Council of China under grants nos. 61135001, 61374023 and 61074179, and the Doctorate Foundation of Northwestern Polytechnical University (CX201320).

7 References

1 Headrick, J.M., Thomason, J.F.: 'Application of high-frequency radar', *Radio Sci.*, 1998, **33**, (4), pp. 1045–1054
2 Shearman, E.D.R.: 'Propagation and scattering in MF/HF ground wave radar'. IEE Proc., 1983, Page 10 of 11, pp. 579–590
3 Sevgi, L., Ponsford, A., Chan, H.C.: 'An integrated maritime surveillance system based on high-frequency surface-wave radars. 1. Theoretical background and numerical simulations', *IEEE Antennas Propag. Mag.*, 2001, **43**, (4), pp. 28–43
4 Abramovich, Y.I., Turcaj, P., Spencer, N.K.: 'Surface wave radar'. United States Patent Application 0142011 A1, July 2003
5 Pulford, G.W., Evans, R.J.: 'A multipath data association tracker for over-the-horizon radar', *IEEE Trans. Aerosp. Electron. Syst.*, 1998, **34**, (4), pp. 1165–1182
6 Torrez, W.C., Yssel, W.J.: 'Over-the-horizon radar surveillance sensor fusion for enhanced coordinate registration'. IEEE Proc. Information, Decision and Control, February 1999, pp. 227–230
7 Weijers, B., Choi, D.: 'OTH-B coordinate registration experiment using an HF beacon'. Proc. Int. Conf. on Radar, 1993, pp. 49–52
8 Pulford, G.W.: 'Over-the-horizon radar multipath tracking with uncertain coordinate registration', *IEEE Trans. Aerosp. Electron. Syst.*, 2004, **40**, (1), pp. 38–56
9 Liu, H., Pan, Q.: 'Comments on 'A multipath data association tracker for over the-horizon radar', *IEEE Trans. Aerosp. Electron. Syst.*, 2005, **41**, (3), pp. 1147–1150
10 Davey, S.J., Gray, D.A.: 'A comparison of track initiation methods with the PMHT'. Proc. Conf. on Information, Decision and Control, 2002, pp. 323–328
11 Willett, P., Ruan, Y., Streit, R.: 'The PMHT: problems and some solutions', *IEEE Trans. Aerosp. Electron. Syst.*, 2002, **38**, (3), pp. 738–754
12 Pulford, G.W., Scala, B.F.L.: 'Over-the-horizon radar tracking using the Viterbi algorithm'. Third Report to High Frequency Radar Division, August 1995, pp. 27–95
13 Liu, H., Liang, Y., Pan, Q., *et al.*: 'A multipath data association for OTHR'. Proc. Int. Conf. Radar, 2006, pp. 1–4
14 Orkun, A.: 'Forecasting of ionospheric critical frequency using neural networks', *Geophys. Res. Lett.*, 1997, **24**, (12), pp. 1467–1470
15 Stanislawska, I., Juchnikowski, G.: 'Generation of instantaneous maps of ionospheric characteristic', *Radio Sci.*, 2001, **36**, (5), pp. 1073–1081
16 Bucknam, J.N.: 'Beacon-assisted vectoring of aircraft with OTH radar'. Rome Lab. Technical Report, RL-TR-94-211, December 1994
17 Jeffrey, L.K., Richard, H.A.: 'Maximum Likelihood coordinate registration for over-the-horizon radar', *IEEE Trans. Signal Process.*, 1997, **45**, (4), pp. 945–959
18 Frazer, G.J.: 'Forward-based receiver augmentation for OTHR'. IEEE Radar Conference, April 2007, pp. 373–378
19 Kong, R., Cheng, Y., Liang, Y.: 'Mode identification and location improvement based on data association of OTHR and azimuth-only sensors', *Acta Aeronautica et Astronautica Sinica*, 2012, **33**, (6), pp. 1061–1069
20 Chen, L.: 'Researches on signal and information processing in over-the-horizon-radar'. Master thesis, Northwestern Polytechnical University, 2011
21 Deb, S., Yeddanapudi, M., Pattipati, K.R., Bar-Shalom, Y.: 'A generalized 2-D assignment algorithm for multisensor-multitarget state estimation', *IEEE Trans. Aerosp. Electron. Syst.*, 1997, **33**, (2), pp. 523–538
22 Popp, R., Pattipati, K., Bar-Shalom, Y.: 'm-best S-D assignment algorithm with application to multitarget tracking', *IEEE Trans. Aerosp. Electron. Syst.*, 2001, **37**, (1), pp. 22–39

23 Bar Shalom, Y.: 'On the track-to-track correlation problem', *IEEE Trans. Autom. Control*, 1981, **26**, (2), pp. 571–572
24 Singer, R.A., Kanyuck, A.T.: 'Computer control of multiple site track correlation', *Automation*, 1971, **7**, (3), pp. 455–463
25 Bar-Shalom, Y., Fortmann, T.E.: 'Tracking and data association' (Academic Press, New York, 1988)
26 Lines, L.R., Treitel, S.: 'A review of least-squares inversion and its application to geophysical problems', *Geophys. Prospect.*, 1984, **32**, pp. 159–186
27 Kang, L., Xie, W., Huang, J.: 'New data association technique based on ACO with directional information considered', *J. Syst. Eng. Electron.*, 2008, **19**, (6), pp. 1283–1286
28 Liang, Y., Cao, J., Zhang, L., *et al*.: 'A biological-inspired sensor wakeup control method for wireless sensor network', *IEEE Trans. Syst. Man Cybern. Part C: Appl. Rev.*, 2010, **40**, (5), pp. 525–538
29 Choo, H., Ling, H., Liang, C.S.: 'Shape optimization of corrugated coatings under grazing incidence using a genetic algorithm', *IEEE Trans. Antennas Propag.*, 2003, **51**, (11), pp. 3080–3087
30 Peterson, C., Anderson, J.R.: 'Neural networks and NP-complete optimization problems: a performance study on the graph bisection problem', *Complex Syst.*, 1988, **2**, pp. 59–89
31 Liang, Y., Feng, X., Yang, F., *et al*.: 'The distributed infectious disease model and its application to collaborative sensor wakeup of wireless sensor networks', *Inf. Sci.*, 2013, **223**, pp. 192–204

doi: 10.1049/iet-rsn.2013.0017